Project 068 Combustor Wall Cooling with Dirt Mitigation

The Pennsylvania State University

Project Lead Investigator

Reid A. Berdanier
Associate Professor
Department of Mechanical Engineering
The Pennsylvania State University
NARCO Building, CATO Park, Room 148
3127 Research Drive
State College, PA. 16801
(814) 863-3972
rberdanier@psu.edu

University Participants

The Pennsylvania State University (Penn State or PSU)

- P.I.s: Prof. Karen Thole, Prof. Reid A. Berdanier, Dr. Michael Barringer, Prof. Stephen Lynch
- FAA Award Number: 13-C-AJFE-PSU-128
- Period of Performance: June 5, 2020, to September 30, 2026
- Tasks:
  1. Manufacturing and testing of combustor liner cooling concepts with small coupons
  2. Testing of scaled models of optimal cooling concepts
  3. Profile simulator for the Steady Thermal Aero Research Turbine (START)

Project Funding Level

For the entire 5-year effort ASCENT Project 068 received $1,400,000 Federal Aviation Administration (FAA) funding, and matching funds of $1,400,000 were provided by Pratt & Whitney ($1,250,000), University of Michigan (U-M) ($100,000) and PSU ($50,000).

Investigation Team

Prof. Reid A. Berdanier (P.I.), Management, reporting, and oversight of all technical tasks
Prof. Karen A. Thole (co-P.I.), Management, reporting, and oversight of all technical tasks
Prof. Stephen Lynch (co-P.I.), Management, reporting, and oversight of all technical tasks
Assoc. Res. Prof. Michael Barringer (research advisor), Task 3
Scott Fishbone (project manager, departed), Tasks 1–3
Tom Houck (project manager), Tasks 1–3
Kyle McFerran (graduate student, PSU, graduated), Tasks 1 and 2
Chad Schaeffer (graduate student, PSU, graduated), Task 3
Fabrizzio Vega (graduate student, U-M), Task 2
Peyton Boudinot (graduate student, U-M), Task 2
Dan Strobel (graduate student, PSU), Task 3
Benjamin Bizzak (graduate student, PSU), Task 3

Project Overview

A critical issue related to the current operation of gas turbines is the ingestion of dirt and other fine particles that lead to dirt buildup and reduced cooling of hot section components, such as the liner walls of the combustion chamber. With increasing need to fly in dirty environments, the criticality of operations in dirty environments is increasing. Modern gas turbine engines typically use a double-walled combustor liner with impingement and effusion cooling technologies, whereby impingement cooling enhances the backside internal cooling, and effusion cooling creates a protective film of

coolant along the external liner walls. Dirt accumulation on the internal and external surfaces severely diminishes the heat transfer capability of these cooling designs. This study also investigates the development of a combustor profile simulator upstream of the START test turbine. Combustor profiles affect turbine performance and durability. As combustor designs evolve, particularly the liner cooling technologies, understanding the impacts on the turbine is important. This study investigates practical designs applied to combustor walls to decrease dirt accumulation and also explores the development of a profile simulator that can replicate relevant temperature and pressure profiles at elevated turbulence levels upstream of a test turbine.

Task 2 – Testing of Scaled Models of Optimal Cooling Concepts

The Pennsylvania State University

Objective

The objective of this task is to produce an effective cooling design for combustor walls that is insensitive to dirt accumulation at existing or lower coolant flow rates. Various parameters such as dirt deposition, flow behavior, and heat transfer effectiveness will be investigated and quantified to compare the efficiency of candidate designs. Improved understanding of the underlying reasons for dirt sensitivity and deposition behavior is also being sought. During this past year, the ASCENT Project 068 team took two primary approaches to the problem: (1) identify the impact of dirt deposition on the cooling performance of a typical double-wall combustor liner and (2) identify a novel geometry to replace the double-wall liner design with a triple-wall combustor liner.

Research Approach

Considering size constraints due to material availability, designs for new combustor liner walls were created and are presented in Figures 1, 2, and 3. In total ten combustion liner walls were designed, including two effusion plates and eight impingement plates. In total there are four diameters of impingement holes, namely D = 0.025, 0.06, 0.09, and 0.125 in., each with two versions of differing wall spacings.

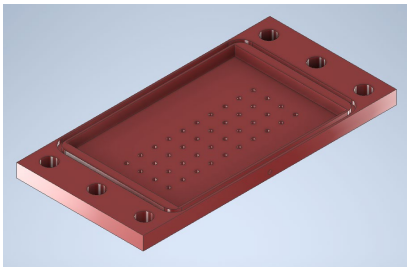

Figure 1. Third-wall impingement plate, with an impingement hole diameter of 0.06 in.

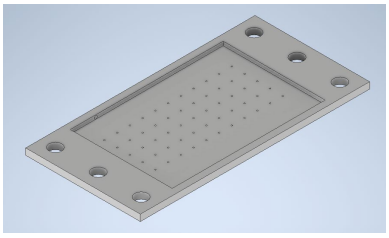

Figure 2. Second-wall impingement plate, with an impingement hole diameter of 0.025 in.

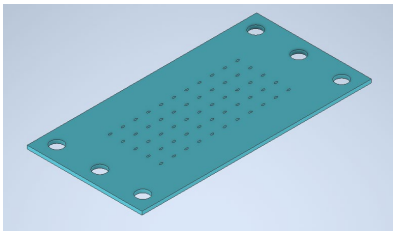

Figure 3. First-wall effusion plate, with an effusion hole diameter of 0.033 in. at an angle of 30°.

Additionally, a new concept for the impingement and effusion hole patterns was created. The previously used hole alignment is presented in Figure 4, black representing the impingement holes on the second wall, red the impingement holes on the third wall, and blue the effusion holes on the first wall. This design features effusion holes laterally and longitudinally offset from the second-wall impingement holes and the third wall impingement holes centered between four second-wall impingement holes. The new design, shown in Figure 5, centers the effusion holes between two adjacent second-wall and two adjacent third-wall impingement holes.

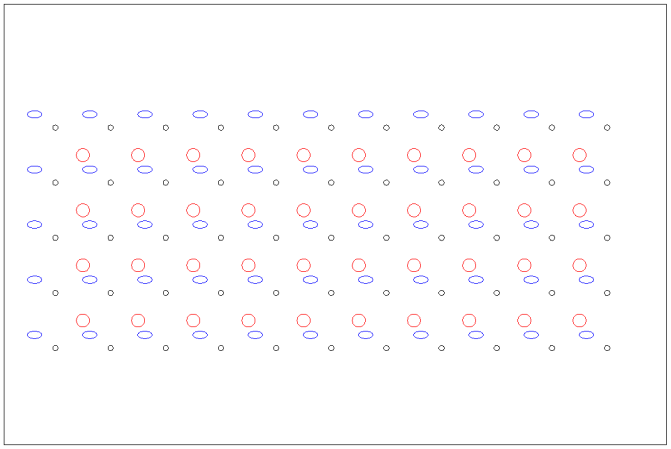

Figure 4. Previously used effusion (blue) and impingement (red, black) hole pattern.

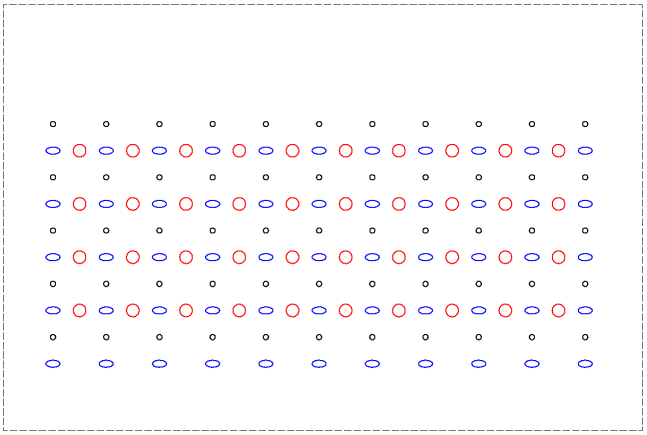

Figure 5. New effusion (blue) and impingement (red, black) hole pattern.

Compilation of Test Matrix

A plan for tests to be conducted at the room- and at the high-temperature test facilities was devised for the original and new hole patterns, as seen in Table 1 and Table 2, respectively. The test matrix for the original hole pattern features previously done hole double- and triple-wall tests, with novel tests for this design being changes in the wall to wall spacing to hole diameter ($\frac{H}{D}$) ratio alternates between 3 and 10. All tests presented in the test matrix for the new hole pattern will be new.

It should be stated that even previously performed room-temperature tests will be repeated at the new U-M facility (i.e., all tests in both matrices will be performed at both temperatures).

Table 1. Test matrix for original hole pattern.

	Wall #0	Wall #1	Wall #2
Double Wall Tests	-	Imp-025-3	Eff-033c0
	-	Imp-025-10	Eff-033c0
Triple Wall Tests	Imp-125-10	Imp-025-3	Eff-033c0
	Imp-090-10	Imp-025-10	Eff-033c0
	Imp-060-10	Imp-025-3	Eff-033c0
	Imp-125-3	Imp-025-10	Eff-033c0
	Imp-090-3	Imp-025-3	Eff-033c0
	Imp-060-3	Imp-025-10	Eff-033c0

Imp-**DDD**-**HH**
DDD ➔ Hole diameter ($\frac{1}{1000}$ths inches)
HH ➔ $\frac{H}{D}$, ratio of plate spacing above to hole diameter

Eff-**DDDs**
DDD ➔ Hole diameter ($\frac{1}{1000}$ths inches)
s ➔ Hole geometry, c: cylindrical

Table 2. Test matrix for new hole pattern.

	Wall #0	Wall #1	Wall #2
Double Wall Tests	-	Imp-025-3	Eff-033c1
	-	Imp-025-10	Eff-033c1
Triple Wall Tests	Imp-125-10	Imp-025-3	Eff-033c1
	Imp-090-10	Imp-025-10	Eff-033c1
	Imp-060-10	Imp-025-3	Eff-033c1
	Imp-125-3	Imp-025-10	Eff-033c1
	Imp-090-3	Imp-025-3	Eff-033c1
	Imp-060-3	Imp-025-10	Eff-033c1

Imp-**DDD**-**HH**
DDD ➔ Hole diameter ($\frac{1}{1000}$ths inches)
HH ➔ $\frac{H}{D}$, ratio of plate spacing above to hole diameter

Eff-**DDDs**
DDD ➔ Hole diameter ($\frac{1}{1000}$ths inches)
s ➔ Hole geometry, c: cylindrical

Construction of Test Facility

The design of the test rig has been completed, a diagram for which is presented in Figure 6. Like the previous rig, this one will be slug-feeding dirt samples into the system.

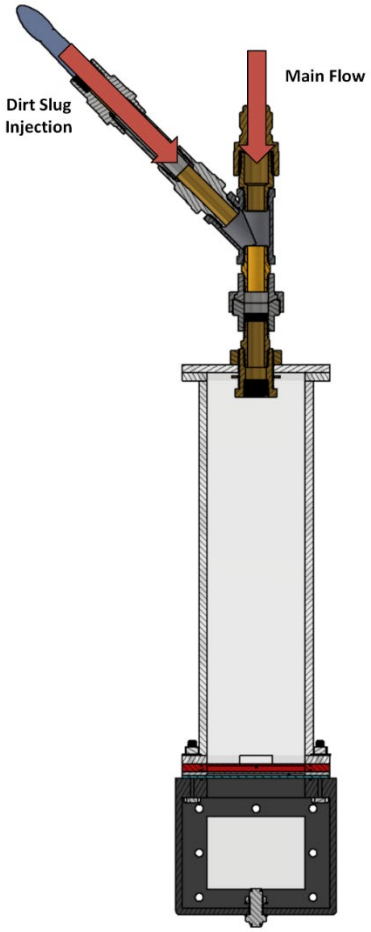

Figure 6. Cross-sectional view of the new U-M dirt rig.

Finally, the as-built flow control plumbing circuit is shown in Figure 7. An Alicat® mass flow controller regulates the flow rate to maintain a constant pressure ratio (PR) of 1.045 across the test section. The mass flow that the controller is set to is updated by the LabVIEW code via a Proportional-Integral-Derivative (PID) system, the process variable being the PR calculated from pressures measured by transducers.

The room-temperature dirt deposition facility at U-M, shown in Figure 8, serves to study the effects of dirt deposition in cooling geometries found within the combustor liner of gas turbines. A test coupon emulating the walls of a combustor liner is composed of stacked impingement and effusion plates. The facility features a slug feed system for injecting dirt into the main flow path. During a typical deposition experiment, a nominal mass of dirt is split into three slugs of equal mass and are sequentially fed into the system. Pressure taps are located at various locations throughout the facility for measuring the coolant air pressure (P_{0C}), pressures between subsequent effusion/impingement plates (P_1, P_2), and the pressure at the exit of the test coupon (P_∞).

® Alicat is a registered trademark of Alicat Scientific, Inc., Tucson, Arizona.

Figure 7. As-built flow control plumbing at U-M.

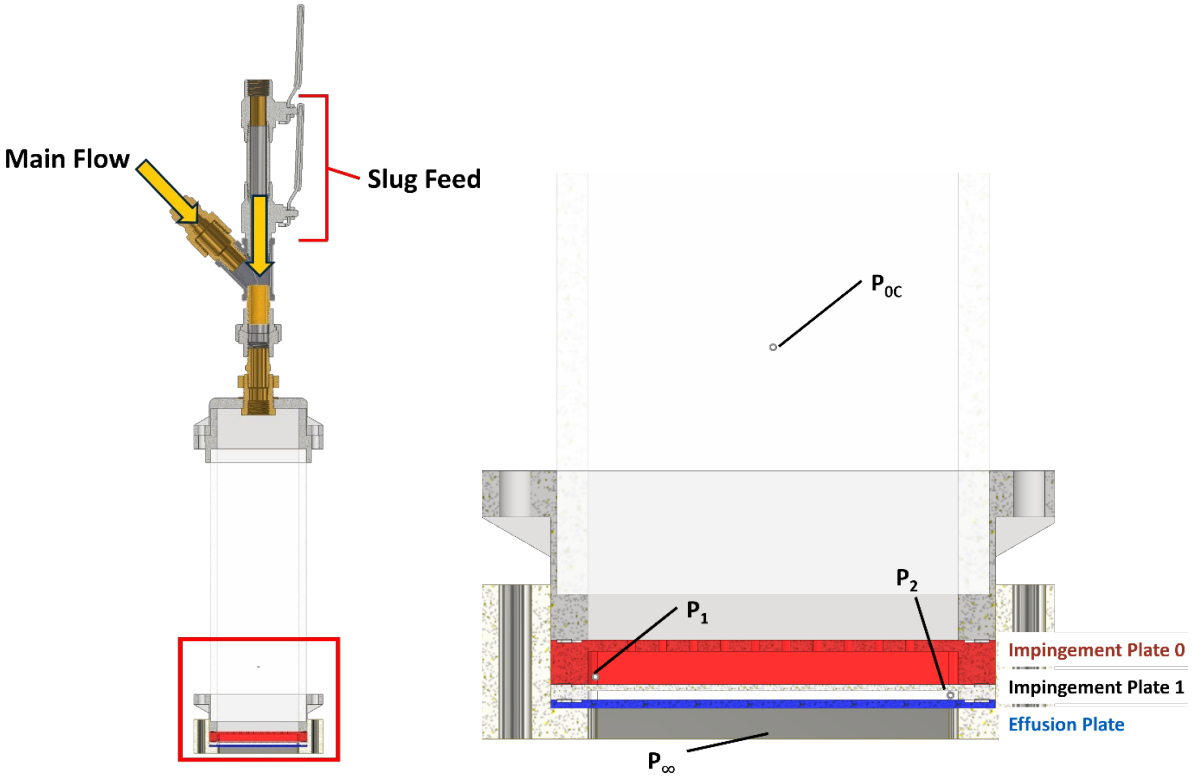

Figure 8. Overview of room-temperature dirt deposition testing facility (left). Cross sectional view of test coupon in testing facility (right).

An absolute pressure transducer measures the pressure of the supply air (P_{Supply}), a differential pressure transducer measures the pressure drop from the air supply to the plenum (ΔP_0), and a second differential pressure transducer with ±0.08% best straight line accuracy measures the pressure drop across the test section (ΔP_{Total}). As per Equation 1, the PR across the test section is dynamically calculated during experiments. A PID controller, using PR as the process variable, maintains a constant PR = 1.045 across the test section by adjusting the mass flow rate of coolant air ($\dot{m}$).

The flow parameter (FP), defined in Equation 2, is also monitored during testing and serves to quantify the flow through the test section. To maintain consistency with previous studies, the metering section of the FP is the "Imp1" plate, with the number of holes (N) and hole diameter (D_1) corresponding to "Imp1." For this particular double-wall geometry, the dependence of the FP with PR under clean conditions (i.e., no dirt injection) is depicted in Figure 9. The FP measured at the start of each experiment, prior to dirt injection, is compared to this baseline curve to make sure that no blockages remain from previous tests.

$$PR = \frac{P_{0C}}{P_{\infty}} = \frac{P_{supply} - \Delta P_0}{P_{supply} - \Delta P_0 - \Delta P_{total}} \quad \text{(Eq. 1)}$$

$$FP = \frac{4\dot{m}\sqrt{RT_{0C}}}{\pi P_{0C} N D_1^2} \quad \text{(Eq. 2)}$$

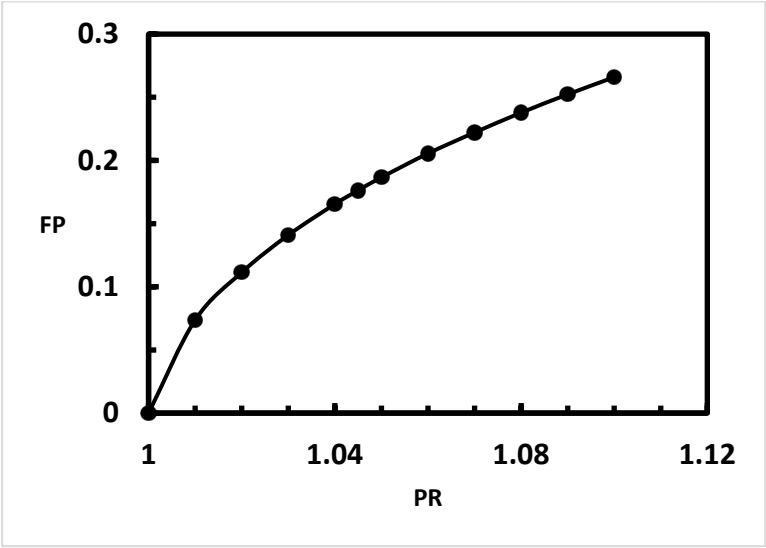

Figure 9. Baseline clean flow parameter (FP) as a function of pressure ratio (PR) for the baseline double-wall geometry.

In collaboration with researchers at the National Aeronautics and Space Administration (NASA) Glenn Research Center (GRC), a facility has been constructed to study deposition within combustor liners at high temperatures. Of particular interest in these experiments is to investigate the enhanced deposition mitigation provided by the addition of a third combustor liner wall. NASA GRC houses a Mach 0.3 burner rig, shown in Figure 10, and is used to simulate the high-temperature conditions within a combustor.

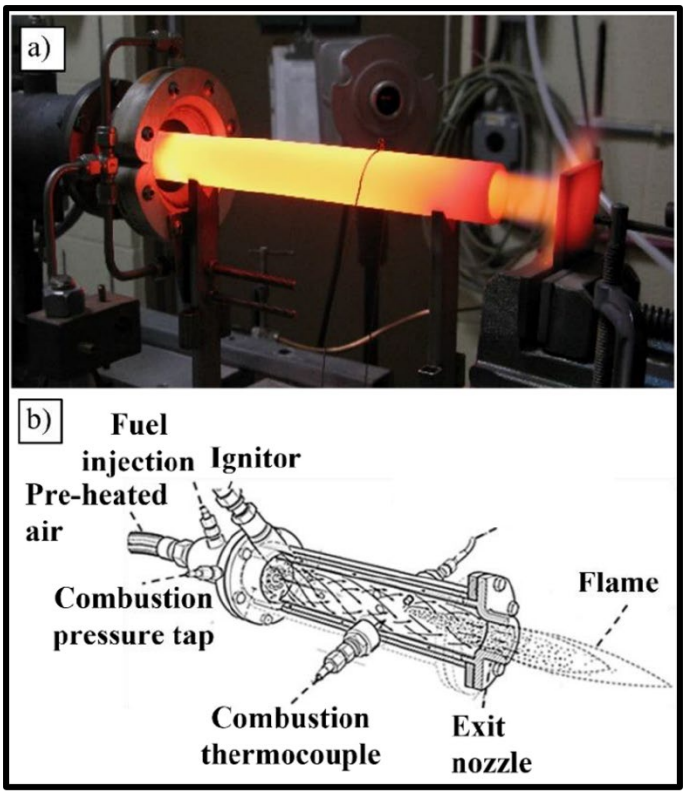

Stokes, J. L. & Presby, M. J. (2024)

Figure 10. (a) The burner rig during operation, heating up a sample. (b) A drawing of the burner rig labeling key components.

A top-down view of the testing rig is shown in Figure 11. Test coupons made up of stacked impingement and effusion plates are used to simulate the walls of a combustor liner and are housed in a stainless-steel enclosure. The enclosure serves to create an airtight seal between adjacent plates by pressing the plates together. Pre-heated particle-laden air is fed into the backside of the enclosure, passes through the test coupon, and exits out of the effusion holes on the other side. An inline heater brings the absolute temperature of the cooling air, T_{0C}, to half of the effusion plate surface temperature (TS). A thermocouple provides the coolant temperature to a furnace controller that regulates the power output of the inline heater to achieve the desired coolant temperature.

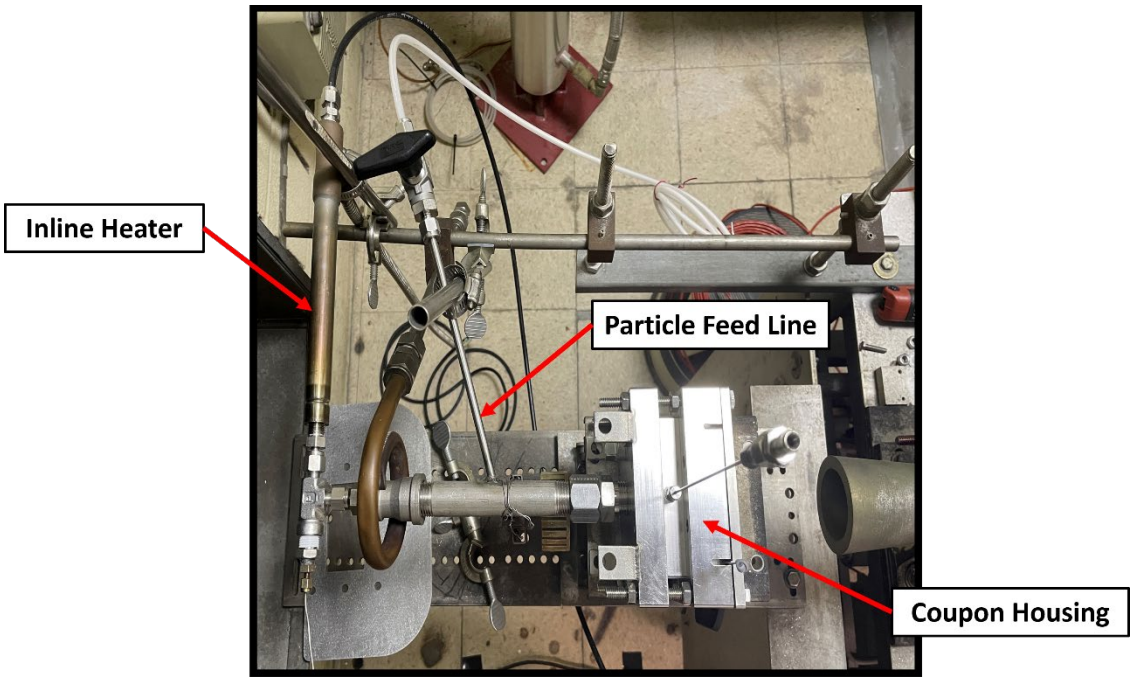

Figure 11. Top-down view of the testing rig.

The burner nozzle was aimed at the combustor side (downstream) of the effusion wall, as seen in Figure 12, with the flame produced having the capability of creating hot side surface temperatures on the effusion wall of up to 1,200°C. At the start of each experiment, the fuel-air ratio for the burner is modified until the desired T_s is reached at steady state. A pyrometer monitors T_s at the center of the effusion wall.

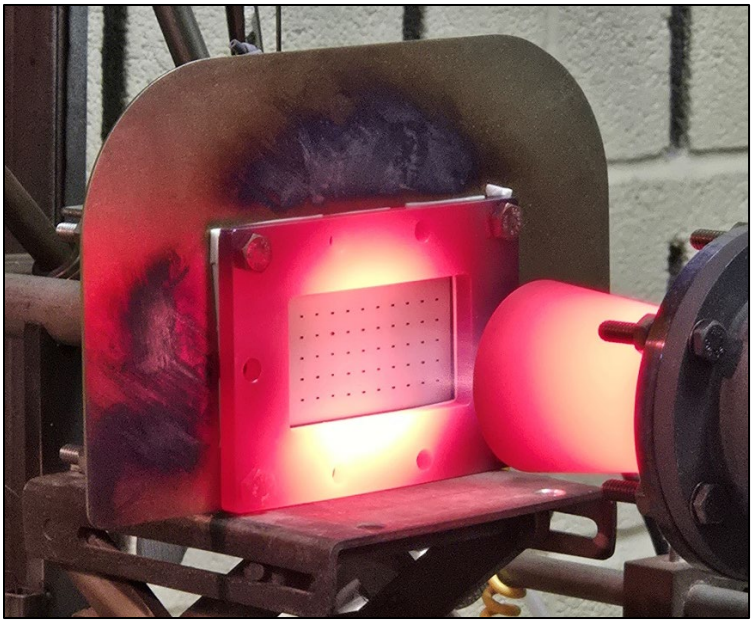

Figure 12. The high-temperature testing facility during operation. An effusion plate (center) is exposed to a flame that is seen coming out of the burner nozzle (right).

A total of four unique test cases are performed varying in combustor liner geometry. The different test cases are presented in Table 3. The combustor liner geometry varies in the number of walls (double- or triple-wall) and in the diameter of the impingement holes on the third wall (D_0). A constant PR of 1.045 is maintained across the liner for each test case.

Table 3. Testing conditions for high-temperature deposition experiments.

	Testing Conditions			Geometry		
	T_s [˚C]	T_{0C} [˚C]	PR [-]	D_0 [in]	D_1 [in]	D_2 [in]
Combustor Liner Geometry	1200	463	1.045	0.060	0.025	0.033
	1200	463	1.045	0.090	0.025	0.033
	1200	463	1.045	0.125	0.025	0.033
	1200	463	1.045	-	0.025	0.033

A thermal barrier coating (TBC) composed of yttria-stabilized zirconia was applied onto all the effusion plates via the process of Plasma Spray-Physical Vapor Deposition (PS-PVD). The average coating thickness for each of the three plates is around 120 microns. As shown in Figure 13, the TBC inadvertently deposited on the inside of the effusion holes. Since this is a common occurrence in effusion plates coated and used by industry, the holes were not cleared out following the coating process.

Figure 13. A hole on an effusion plate coated in yttria-stabilized zirconia thermal barrier coating.

Throughout every test, the PR across the test coupon (PR), defined as the ratio of coolant pressure immediately upstream (P_{0C}) to that immediately downstream, is maintained constant at PR = 1.045. Because the test coupon vents to atmosphere, the pressure immediately downstream to it is taken to be the absolute ambient pressure (P_∞) for which a barometer inside the burner rig cell is referenced at the start of every test. An OMEGA 2.5 psi differential pressure transducer measures the drop in pressure of the coolant across the test coupon (ΔP_{Total}). The PR is calculated in terms of P_∞ and ΔP_{Total} as per Equation 3.

$$PR = \frac{P_{0C}}{P_\infty} = 1 + \frac{\Delta P_{total}}{P_\infty} \quad \text{(Eq. 3)}$$

Building supply compressed air serves as the coolant in these series of tests and is regulated throughout their duration by a mass flow controller (250 SLPM Flow Controller, Alicat Scientific, Inc.) such that a PR=1.045 is maintained across the test coupon. After passing through the mass flow controller, the air is heated to the desired coolant temperature (T_{0C}) using a 750W inline heater, the temperature of which is measured with a type-K thermocouple placed at the outlet of the heater. To maintain a constant T_{0C}, a temperature controller regulates the power output of the heater. All piping downstream to the inline heater is insulated with mineral wool.

The coolant flow was seeded with AFRL-05 (Air Force Research Laboratory) particles which is primarily made up of gypsum and quartz and has a mean particle diameter of 1.2μm with a 0-3μm size distribution. Dust feed was accomplished via a slug injection system where a discrete quantity of dirt was fired into the coolant flow. Prior to use in testing, dirt samples were passed through a fine wire mesh to break up agglomerations and subsequently dehumidified by baking in an oven.

Prior to and after deposition, the mass of each impingement and effusion plate that made up the test coupon was individually measured. The difference between corresponding measurements indicated the mass of dirt that deposited on the n^{th} layer (m_n). The primary method for comparing dirt deposition across liner geometries was through the capture efficiency (η_c) presented in Equation 4. The capture efficiency of the n^{th} layer is defined as the ratio of m_n to the total dirt which deposited on layers downstream to the first impingement plate (m_t). Because the double-walled configuration has only one impingement plate, by definition its capture efficiency is always 100%, whereas for a triple-wall configuration the capture efficiencies for the middle impingement and the effusion plates both sum to 100%.

$$\eta_c = \frac{m_n}{m_t} * 100 \qquad \text{(Eq. 4)}$$

Capture efficiencies for the baseline double-wall design and the best performing triple-wall design are presented for T_s = 1,200°C and for room temperature conditions in Figure 14. Under high temperature conditions, the presented triple-wall design is shown to reduce dirt deposition on the effusion wall by 63%. These results agree with those by McFerran et al. (2025) who reported an 87% reduction of deposition on the effusion wall using the same combustor liner design. It is well known that deposition is more likely to occur at higher temperatures, which explains the smaller reduction seen under high temperature conditions. Both room- and high- temperature results support the idea that the addition of an impingement wall to the commonly seen double-wall configuration will significantly reduce deposition on the effusion wall.

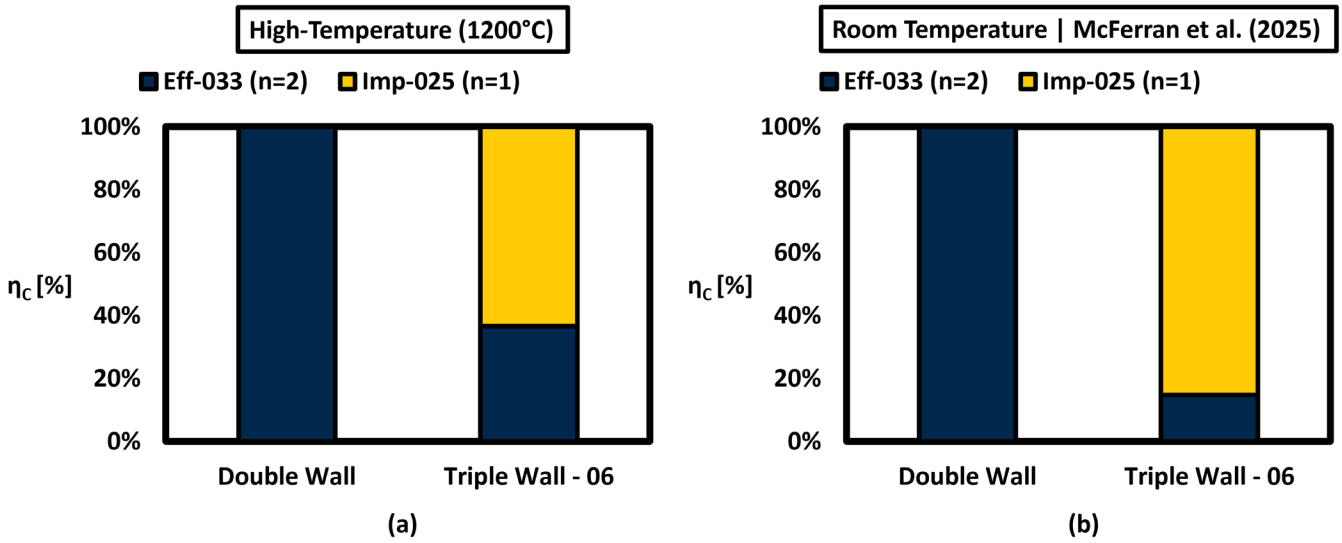

Figure 14. Dirt capture efficiencies for the double-wall configuration and triple-wall configuration, with Imp-060 (n=0), for (a) high effusion wall surface temperature and (b) room temperature conditions.

An optical profilometer was used to take three-dimensional scans of resulting dirt depositions after every test. The lateral average of the height profiles for the middle three columns of dirt mounds on the effusion wall is presented for the double- and triple-wall configurations in Figure 15. For both cases, the mounds form in the stagnation region of the

impingement jets from the plate immediately upstream to the effusion wall. Also, in agreement with the capture efficiency results, the lateral average of deposit heights is smaller when using a triple wall over a double-wall configuration indicative of a reduction in deposition on the effusion wall.

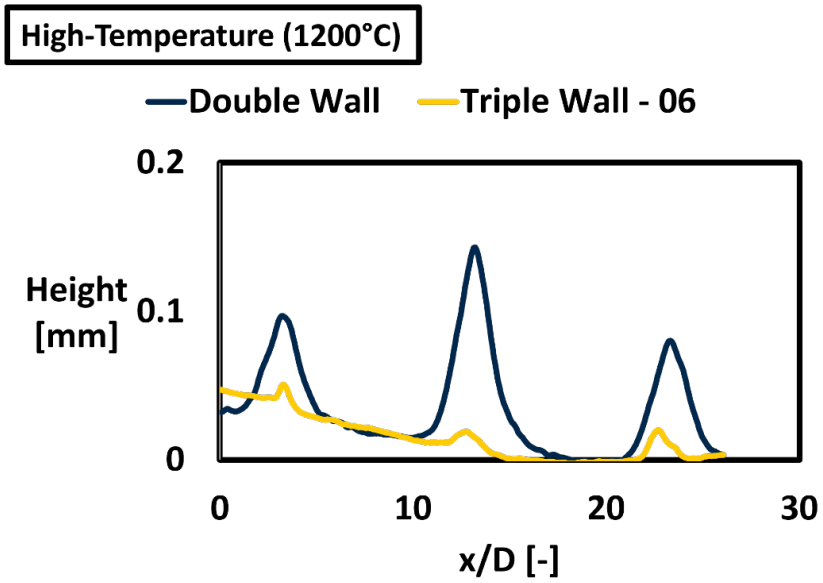

Figure 15. Lateral average deposit heights on the effusion wall for double- and triple-wall liner geometries.

Task 3 – Profile Simulator for START

The Pennsylvania State University

Objectives

The objectives of this task are to (1) develop and integrate a non-reacting profile simulator to be placed upstream of the START test turbine and (2) understand the impacts of a range of temperature and pressure profiles, representative of current and future combustors, on turbine efficiency and durability.

Background

A combustor profile simulator was designed and is being implemented into the START rig upstream of the turbine test section. Previous reports include a summary of the simulator design, results of initial computational fluid dynamics (CFD) simulations, and the CFD Design of Experiments (DOE) sensitivity analysis. The primary hardware components of the simulator have completed the manufacturing process. During the current reporting period, work was performed to procure all remaining parts that are needed for experimentally testing the simulator, such as the 360° traverse components, flow valves, flow meters, and general instrumentation. An instrumentation plan was developed to establish (1) a bill of materials for the instruments and sensors, (2) details related to instrumentation installation and placement, and (3) details related to egress of sensor tubes and wires. The instrumentation includes temperature, pressure, and flow measurement devices placed throughout the simulator device to control experimental operation settings that enable the simulator to produce the target profiles. In addition, these measurement instruments help aid in CFD validation by providing accurate experimental data that can be compared back to computational predictions.

Computational Simulations of the Profile Simulator

Recall from previous reports, the design target profiles for the new profile simulator include a radial center-peaked, outer diameter (OD) peaked, inner diameter (ID) peaked, and a flat uniform profile. The profile results from the CFD DOE study that best matched the design targets are plotted in Figure 16 and are designated as “Center-Peaked,” “ID-Peaked,” “OD-Peaked,” and “Uniform.” These four target profiles are representative of the engine profiles that were collected from

literature and are also shown. The shaded gray region in Figure 16 represents the full range of profiles produced by the CFD study.

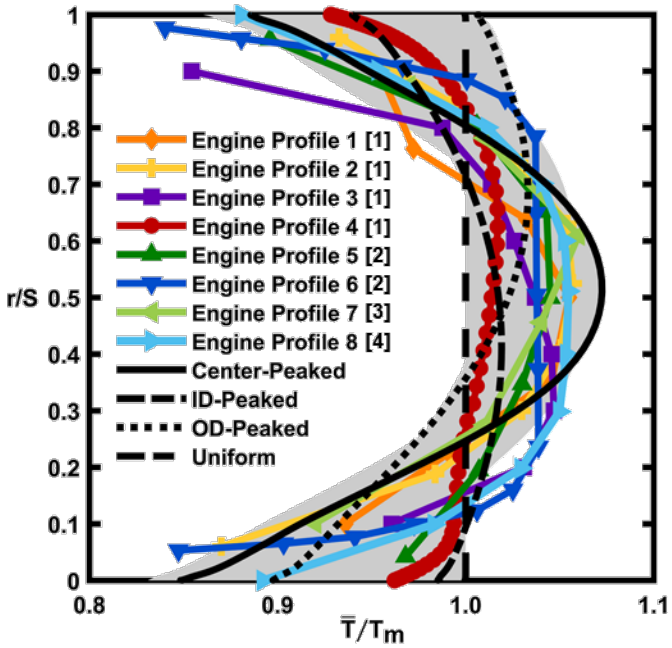

Figure 16. Range of non-dimensional total temperature profiles generated from the CFD DOE, plotted versus radial span location and compared to original equipment manufacturer (OEM) engine combustors (Schaeffer, 2025). ID: inner diameter, OD: outer diameter.

One reason for the selection of the four target profiles was to allow the target profiles to be studied using experiments and a higher fidelity computational model. It was previously determined in literature that the Reynolds-averaged Navier Stokes (RANS) model provides a good prediction of the flow physics, such as jet penetration depth and bulk-averaged velocities, but Large Eddy Simulation (LES) modeling is needed to accurately capture the turbulence created by the intense mixing process of the dilution jets. Understanding how well the RANS simulations predict the temperature profiles is important in determining the viability of using RANS as a predictor for the various flow and geometry configurations in which the profile simulator can be operated. The center-peaked profile was selected as the preliminary case to perform the LES modeling used in this study.

Before transitioning the simulator computations over to LES, a more in-depth RANS simulation was completed that included the domain regions defined by the simulator's upstream strut, profile plate, and downstream turbine vane. An in-depth discussion about the combustor simulator RANS simulation was included in previous reports but a summary of the additional geometry add-ons is provided here as a reminder. The turbine vane used is from the Penn State National Experimental Turbine (NExT) geometry. This updated CFD domain can be seen in Figure 17, with the axial location of the turbine inlet traverse rakes marked in green and the axial location of the vane leading edge (LE) marked in blue. The perforated profile plate acts to reduce the air pressure to enable proper injection of the dilution and effusion flows into the central chamber. The profile plate is interchangeable and contains an engineered perforated pattern that facilitates the desired air mass flow distribution throughout the simulator. In addition to creating a pressure loss, the profile plate is used to reduce the aerodynamic wake effect of the strut's presence in the main flow and to create a uniform flow field entering the central chamber. The struts act as a passageway to distribute cooling air to the inner diameter annulus flow paths and to structurally support the inner hardware components.

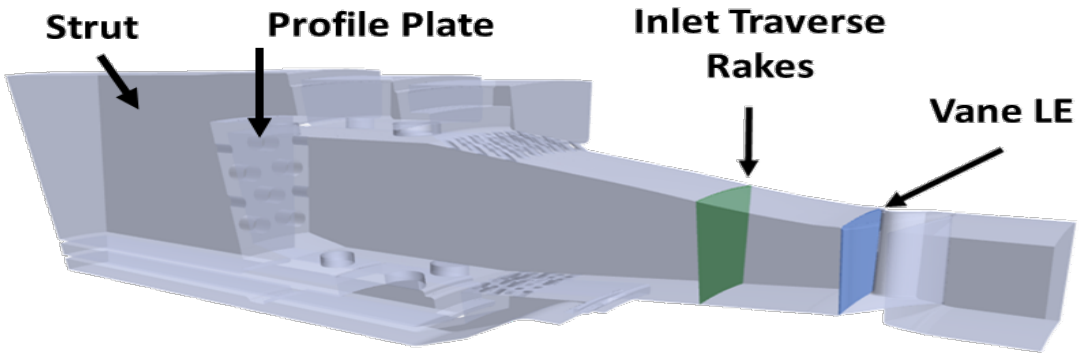

Figure 17. Combustor simulator computational fluid dynamics (CFD) domain including the upstream strut region, profile plate, and downstream turbine vane (Penn State National Experimental Turbine [NExT]). LE: leading edge.

The findings of the RANS simulation are explained in detail in a previous report. With the RANS simulation completed, the transition process from RANS to LES began during the current reporting period. The mesh used for the initial LES simulation was the same mesh that was used for the RANS simulation. The grid resolution for the LES was assessed and selectively refined by evaluating the amount of the turbulent kinetic energy (TKE) that has been resolved to that of the total amount of TKE in a given cell. This ratio is defined as M, as shown in Equation 5.

$$M = \frac{TKE_{resolved}}{TKE_{resolved}+TKE_{sub\ grid\ scale}} \quad \text{(Eq. 5)}$$

The variable $TKE_{sub\ grid\ scale}$ is provided as a field function in the simulation software STAR-CCM+, but $TKE_{resolved}$ is calculated through the unsteady time traces of the velocity field, by summing up the square of each root mean square of the three velocity components and dividing by 2, as shown in Equation 6.

$$TKE_{resolved} = \frac{1}{2}\left(u'_{rms}{}^2 + v'_{rms}{}^2 + w'_{rms}{}^2\right) \quad \text{(Eq. 6)}$$

From literature, Pope (2000) proposed a guideline for performing LES in which he suggested that ideally, $\overline{M} \geq 0.8$, where $\overline{M}$ is defined as the volumetric average of M over the domain. The LES was initialized from the RANS computational grid and solution. An appropriate timestep was determined after the LES solution had been initialized and so that the convective Courant number was never greater than unity. The M criterion was assessed after one flow field time and was determined to need extra refinement in the central chamber, in the approach flow plenums, and in the profile plate region. A flow field time is defined by dividing the total domain length by the volume-average axial velocity as calculated from the RANS simulation. Since the mesh was determined to be under-refined, the domain was re-meshed and evolved through several meshing iterations until the volume average M in the regions of interest were above the $\overline{M} \geq 0.8$ guideline. The mesh cross-section shown in Figure 18a corresponds to a mid-passage plane and was the selected mesh to proceed with the LES because the mesh met the M criterion guideline. Figure 18b shows contour levels of the M criterion within the mid-passage plane of the domain. It can be seen in the regions of interest, particularly the dilution holes, effusion holes, and the central chamber the M criterion is above 0.8. This mesh that was selected for the LES has a volume average M criterion of 0.96.

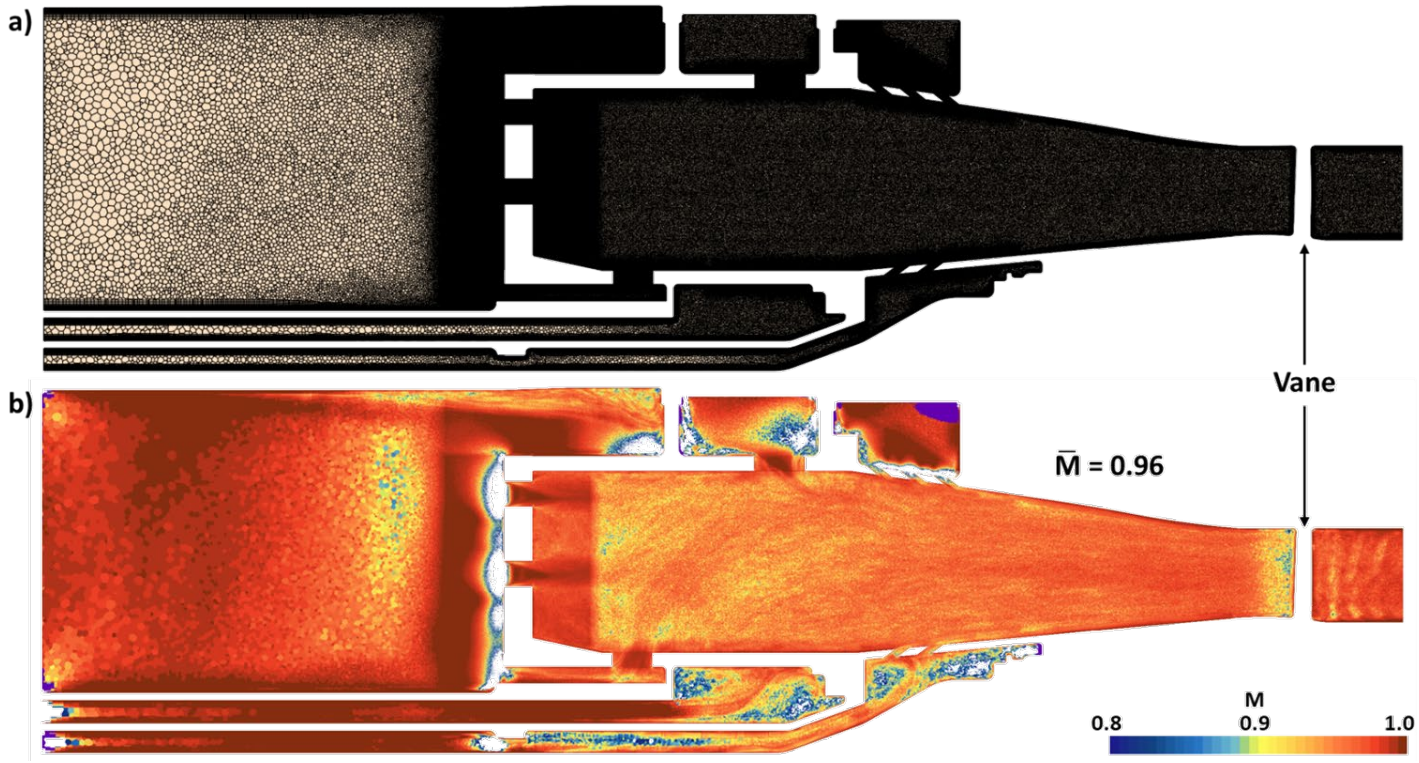

Figure 18. Mid-passage cross-section of the combustor simulator computational fluid dynamics (CFD) Large Eddy Simulation (LES) including (a) mesh domain with extra refinement in high shear zones and coarser regions that are at slow air velocity and (b) M criterion after one flow field time.

The LES was run for a total of seven flow field times, with the first three to ensure at the start of time-averaging the simulation is considered statistically stationary. The LES was time-averaged over four flow-field times ensuring high resolution of the unsteady behavior created by the dilution and effusion flows. Upon the completion of the simulator LES, an analysis was performed that focused on the flow and thermal fields. A comparison was made between the CFD DOE RANS "Center-Peaked" profile, the "more complex" RANS simulation, and the LES simulation radial total temperature profiles to see the prediction capability of RANS compared to the higher fidelity LES. Further analysis included how the LES model predicted temperature and velocity streamwise contours. A deep dive into the hot streaks that exist and were predicted by the LES was important to analyze as well. The hot streaks are known to cause degradation issues on the downstream turbine components and knowing how dilution holes can be used to mix out the hotspots is important. Finally, since LES is known to be better at predicting turbulence over RANS, an analysis focused on turbulence levels was completed.

Computational Simulations of the Shrager Study

Recall the intent as explained in previous reports was to first validate the modeling methods for running both RANS and LES simulations. To validate the modeling methods, both RANS and LES simulations were run that used the same combustor liner geometry as reported by Shrager et al. (2019a). After the computational simulations were completed, a comparison between the predicted RANS and LES flow field and the experimental measurements taken by Shrager was completed. The outward facing effusion hole geometry as seen in Figure 19 was the selected test case for validation, which includes the highest dilution jet momentum flux ratio of I = 30 and a low freestream turbulence intensity of TI = 0.5%.

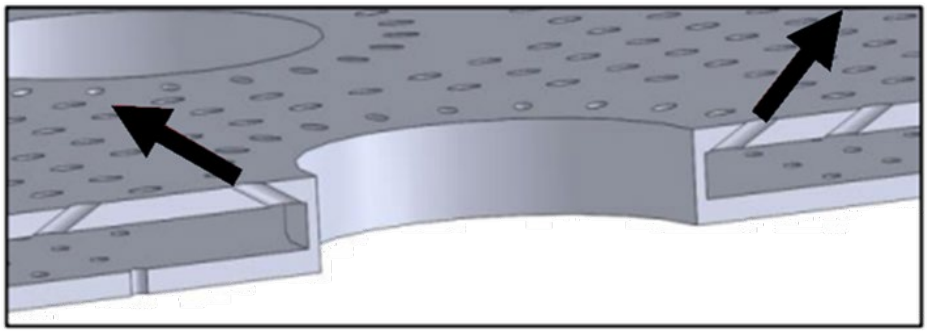

Figure 19. The combustor liner geometry used in the experimental study by Shrager et al. (2019a) showing the large dilution hole with surrounding effusion holes pointing radially outward, that was also used in the current computatonal simulations to validate modeling methodology.

In general, the turbulence levels were underpredicted for five of the six turbulence models that were evaluated. The five turbulence models included the realizable k-ε, the k-ω Menter shear stress transport, the elliptic blending Reynolds stress, the linear pressure strain Reynolds stress, and the incompressible realizable k-ε models. The only model that overpredicted the turbulence intensity was the standard k-ε model. The realizable k-ε model is the same RANS turbulence model that was used in the simulations of the combustor profile simulator. The computational predictions showed that the incompressible turbulence model matched well with the realizable k-ε turbulence model. Overall, the realizable k-ε model compared the best to the experimental results. Figure 20 shows the six different RANS models that were selected and compared to the experimental results collected by Shrager et al.(2019a).

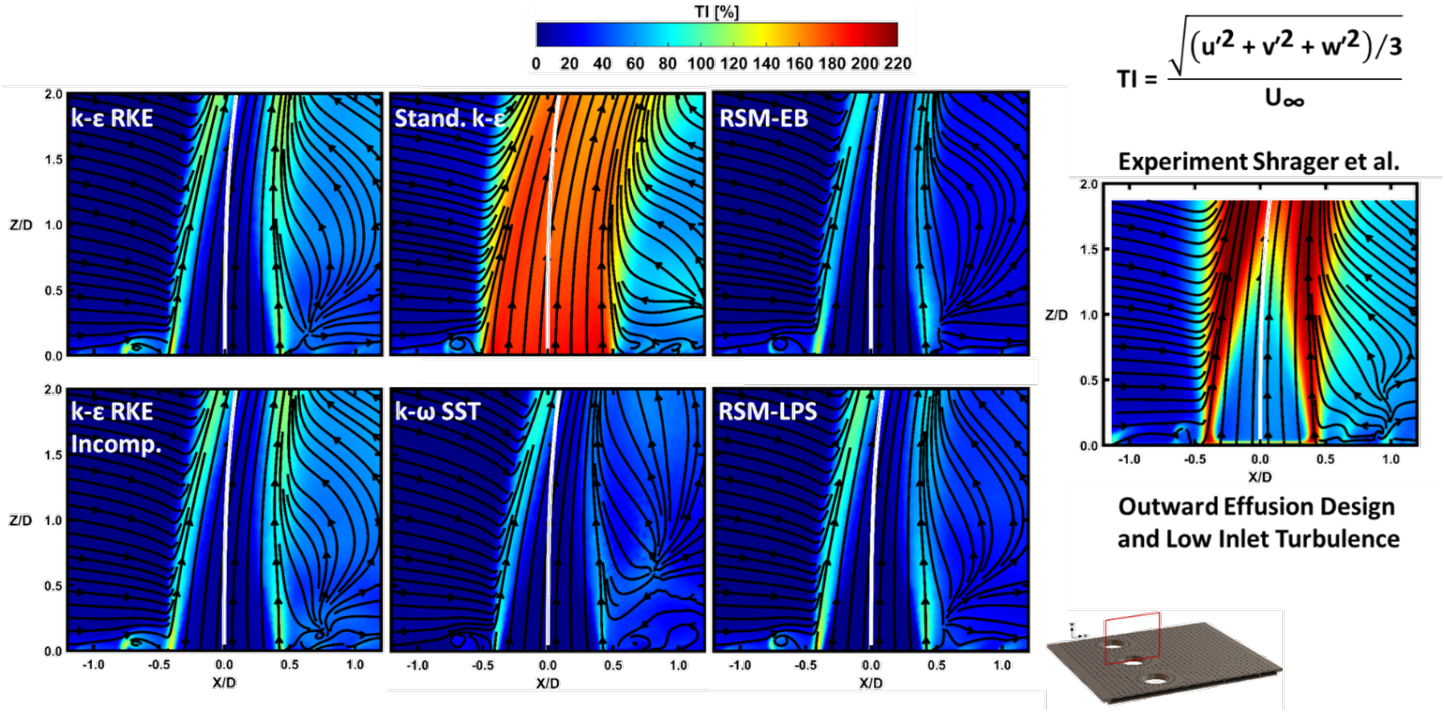

Figure 20. Turbulence intensity contours aligned with the centerline of the central dilution jet comparing six Reynolds-averaged Navier Stokes (RANS) turbulence models of the dilution flow, including k-ε realizable k-e (RKE), standard k-ε, k-ω Shear Stress Transport (SST), EB-RSM (Remote Sensor Module), LPS-RSM, incompressible k-ε RKE, to Shrager's experimentally measured results. TI: turbulence intensity.

Figure 21 shows the results from both the RANS and LES models, including colored streamlines in Figure 21A and contour plots of turbulence intensity levels with streamlines in Figure 21B. The selected RANS model for comparison is the realizable k-e (RKE) model. In Figure 21A the streamlines colored green correspond to the dilution flow, while streamlines colored red correspond to the effusion flow and streamlines colored blue correspond to near-dilution hole effusion flow. Streamlines are shown from the center of each effusion hole, where some of the effusion flow is shown to be entrained up into the dilution flow and mixes with the outer shear layers of the dilution jet. Both the RANS and LES results show this entrainment process, but the LES predicts more entrainment in the region downstream of the dilution hole, which in turn influences the downstream temperature profile shape. In Figure 21B the LES results showed better turbulence predictions than the RANS model compared to the experiment, but both models still slightly underpredicted dilution jet penetration as shown by the white line defined by the Lefebvre correlation.

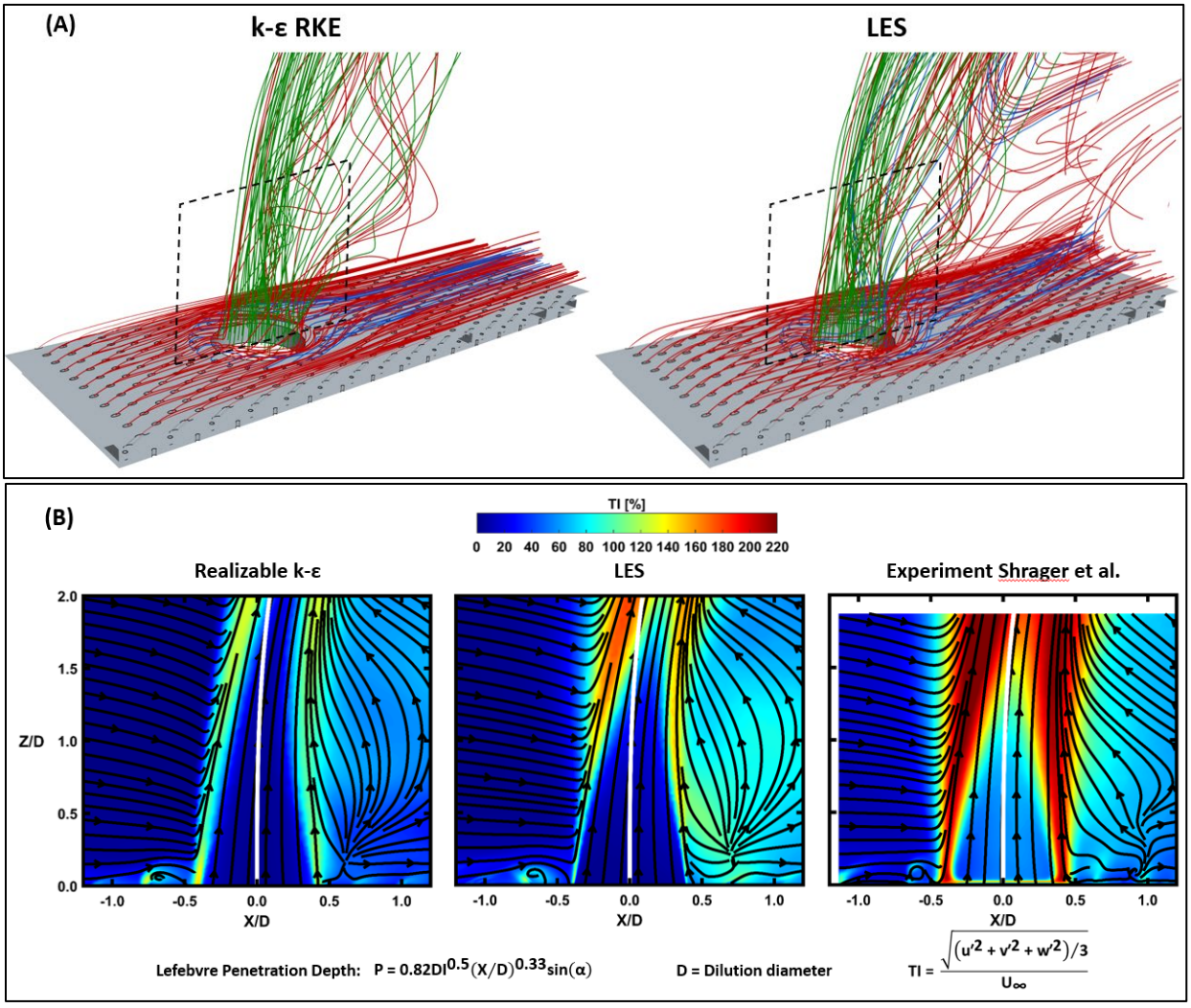

Figure 21. Current computational simulation results from Reynolds-averaged Navier Stokes (RANS) and large eddy simulation (LES) performed at Penn State Steady Thermal Aero Research Turbine (START) compared to previous experimental data from Shrager et al. (2019a) all using the same combustor liner panel geometry with effusion cooling and dilution flow. Results illustrated in (A) show streamlines color coded to the effusion flow (red), near-dilution hole effusion flow (blue), and dilution flow (green). Results illustrated in (B) show contours of turbulence intensity within the dashed planar region passing through the dilution hole. RKE: realizable k-e, TI: turbulence intensity.

To help facilitate experimental testing of the combustor profile simulator within the PSU START rig, specific rig hardware components were pursued for duplicate manufacturing. Figure 22 shows a cross-section drawing of the combustor profile simulator highlighting two rig regions in which hardware manufacturing was pursued to enable the simulator hardware assembly to become a single independent module. These specific hardware components included a forward bulkhead and a cooling air manifold. Once manufactured, these two components will be installed into the combustor profile simulator assembly to quickly support turbine testing with or without the simulator depending on the test goals.

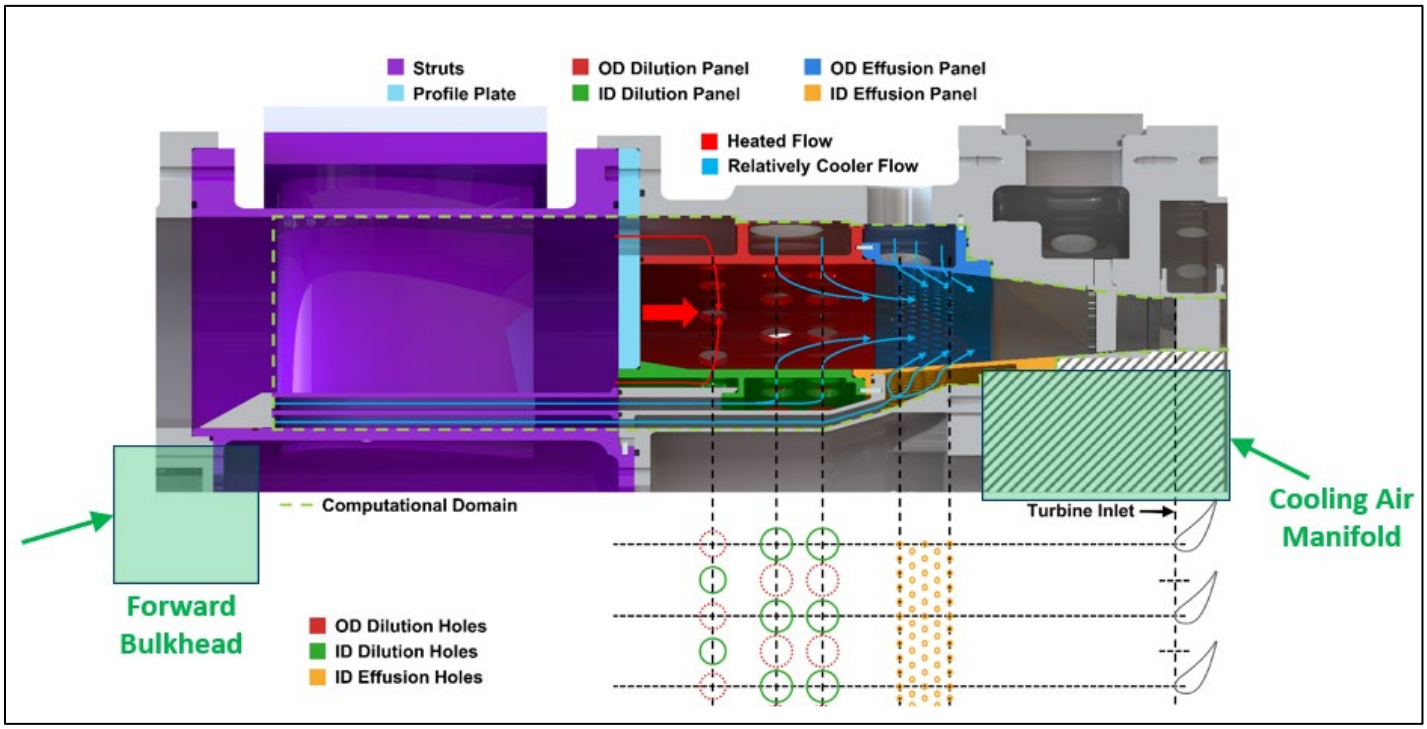

Figure 22. Cross-section drawing of the combustor profile simulator indicating key design features and two highlighted green regions in which hardware manufacturing was pursued to enable the simulator hardware assembly to become a single independent module. ID: inner diameter, OD: outer diameter.

The LES computational modeling of the combustor profile simulator was also completed for the center-peaked target profile case. A total of seven flow through times were completed with the last four flow through times being time averaged. One flow through time is the duration that a particle on average takes to travel from the inlet to the exit of the domain. The mesh grid resolution was assessed and refined by evaluating the ratio of turbulent kinetic energy resolved relative to the total amount of kinetic energy in a given cell. Figure 23 shows a contour plot of its distribution throughout the simulator domain, which contains over 200 million cells. Most of the domain shown in Figure 23 indicates the turbulence to be well resolved above M > 80%, with only a few minor regions to be under resolved including just upstream of the profile plate and areas within the plenums that do not significantly affect the flow and thermal fields within the central chamber of the combustor profile simulator.

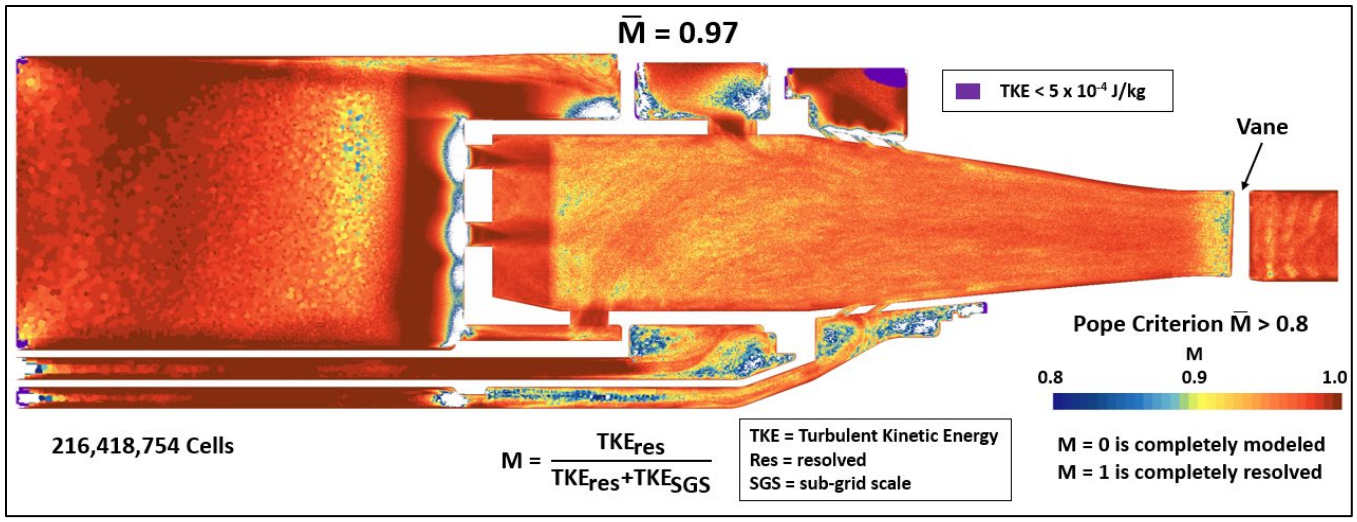

Figure 23. Time-averaged large eddy simulation (LES) contour plot of the turbulence M criterion within the vane mid-passage plane showing successfully resolved turbulence between the ranges of 80% to 100%.

Flow streamlines were also generated from the LES results and are shown in Figure 24. The streamlines are associated with the dilution and effusion flow within the center chamber and were used to illustrate and better understand the fluid mechanics behavior of the individual flow field components. The first-row dilution flow on the OD side of the central chamber is colored red, while the ID side is colored green. Recall, the second-row dilution was not used for the current study. The third-row dilution flow on the OD side is colored yellow, while on the ID side is colored light blue. The liner effusion flow on the OD side is colored dark blue, while on the ID side is colored orange. The streamline trajectories illustrate that the first-row dilution flow penetrates deep into the central chamber freestream and ultimately migrates to a radial height region at the simulator exit plane mostly towards mid-span as intended. The ID effusion and OD effusion flows remain relatively close to their respective liner walls also as intended. The third-row dilution flow on the ID and OD sides penetrate into the central chamber from their respective liner walls a smaller distance than the first row and contributes to the exit temperature profile shape in the radial height regions between mid-span and the near-walls also as intended.

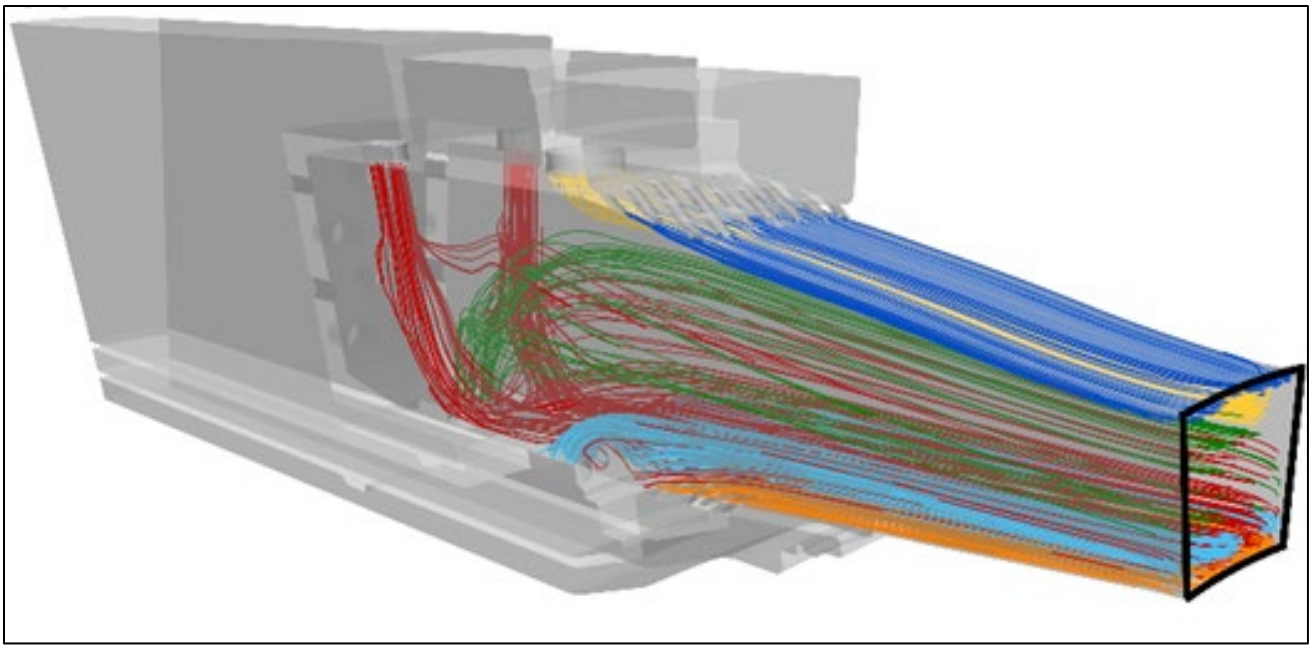

Figure 24. Time averaged large eddy simulation (LES) streamlines within the combustor simulator for the center-peaked target profile.

A new publication was completed on these comparisons (see products section), and a summary of the new paper was made into a poster that was presented at the American Society of Mechanical Engineers (ASME) Turbo Expo 2025. LES computational simulations of the combustor simulator were also completed during the current reporting period including high fidelity predictions of the flow and thermal fields based on the "Center-Peaked" profile configuration. A second new publication was also completed that focuses on the combustor simulator LES methodology and results (see products section). The PhD student working on this aspect of the project wrote two new publications related to the research work and successfully passed his final PhD defense enabling their graduation.

Finally, during the current reporting period, a series of grommet inserts shown in Figure 25 were designed to enable different dilution hole diameters to be used and studied. The threaded inserts act as bushings to change the hole diameter size, and the insertion tool acts as a spanner socket wrench to fasten the insert into the threaded dilution holes. Pricing to manufacture the grommet inserts and tooling was also obtained to pursue manufacturing.

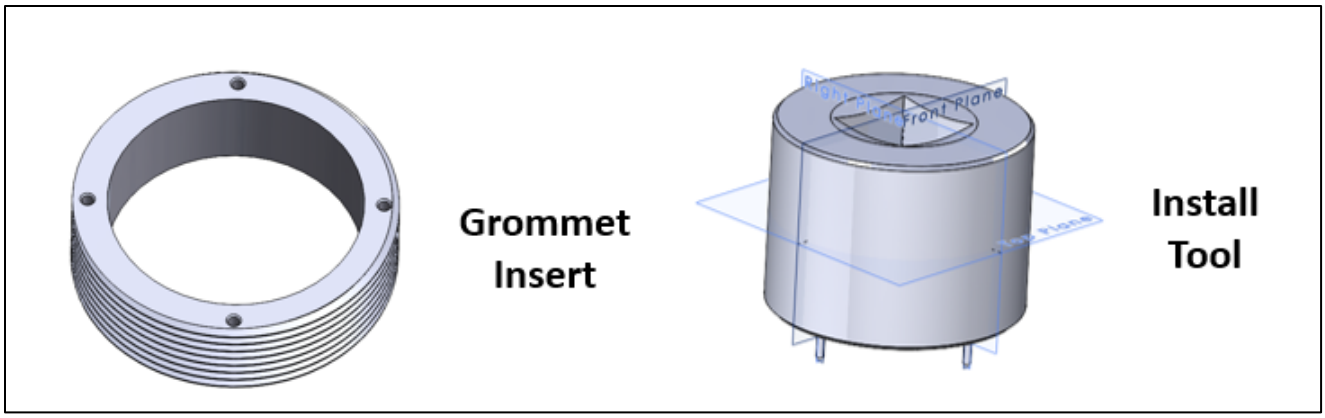

Figure 25. Drawings of an example threaded grommet insert and installation tool that will enable different dilution hole sizes to be installed and studied within the combustor profile simulator.

To help facilitate experimental testing of the combustor profile simulator within the PSU START rig in 2026, specific rig hardware components completed manufacturing. Figure 26 shows a cross-section drawing of the combustor profile simulator highlighting in green the hardware that completed manufacturing helping to enable the simulator hardware assembly to become a single independent module. The hardware highlighted in yellow was assembled and then machined to ensure design intent positional tolerances are met for the hardware closest to the turbine.

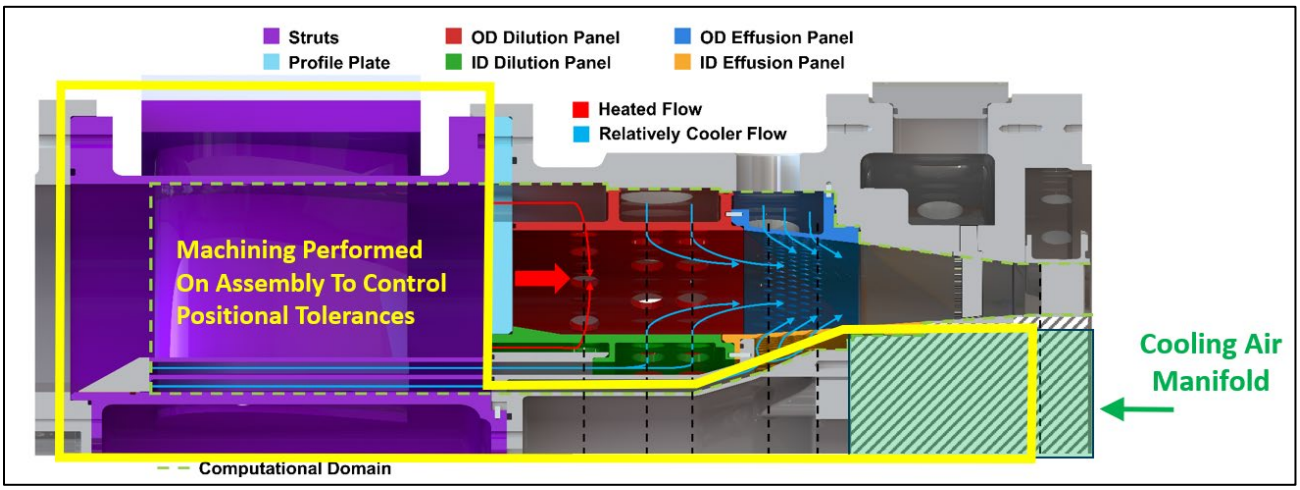

Figure 26. Cross-section drawing of the combustor profile simulator indicating two highlighted regions in which hardware manufacturing was completed to help enable the simulator hardware assembly to become a single independent module and accurately align with the turbine hardware. ID: inner diameter, OD: outer diameter.

The profile plate shown in cyan blue within Figure 26 was originally designed and manufactured to produce the "Center-Peaked" target profile exiting the combustor simulator and entering the test turbine. This profile plate hardware component is shown in Figure 27 and includes a perforation pattern (not shown) that is specific to the target turbine inlet profile. Efforts began to design and manufacture additional profile plates for the other target profiles shown in Figure 27 referenced within the red box.

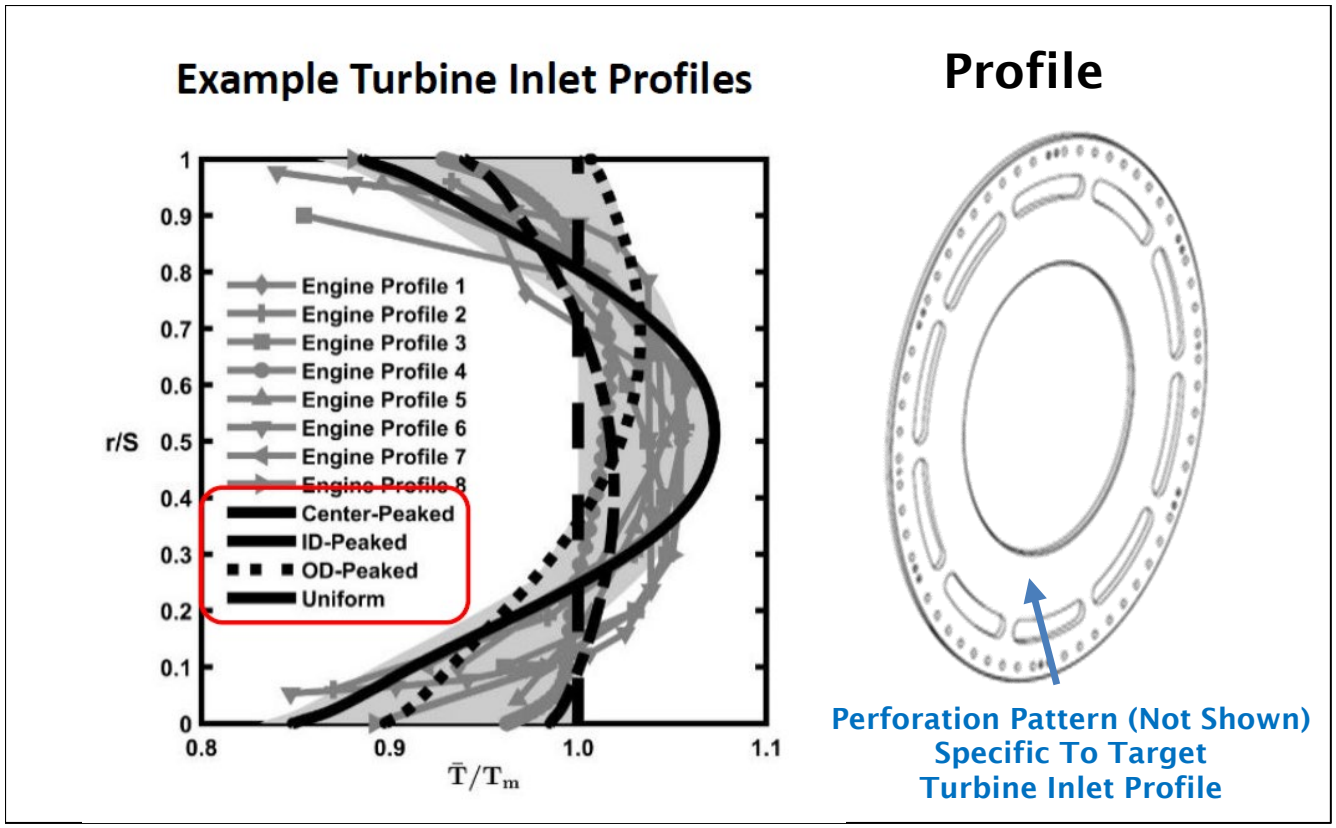

Figure 27. Drawing of the profile plate located at the inlet of the combustor simulator central chamber that is designed with a perforation pattern specific to the target turbine inlet profile. ID: inner diameter, OD: outer diameter.

Finally, during the current reporting period trial assembly work continued for the complete 360° traverse system that is located at the exit of the combustor simulator shown in Figure 28. This traverse system includes a series of rake probes that enable the flow temperature and pressure exiting the simulator and entering the test turbine to be spatially measured around the full annulus. Planning was also initiated for integrating the instrumentation shown within the combustor simulator assembly.

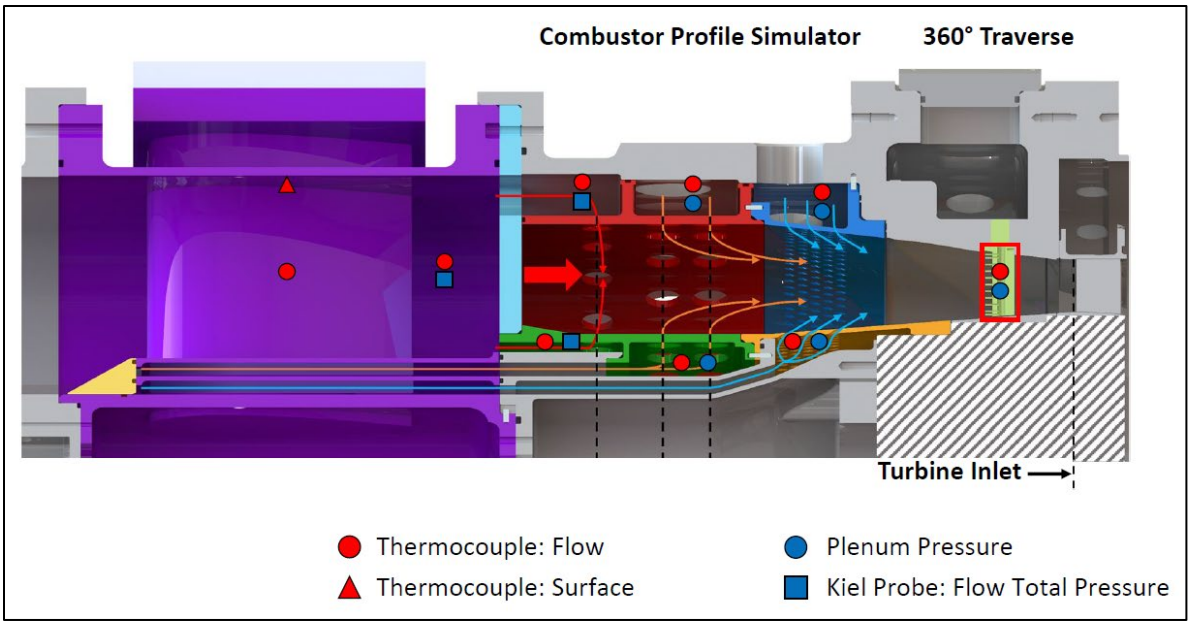

Figure 28. The traverse system at the combustor simulator exit will be used to measure the spatial profiles of temperature and pressure entering the turbine, while the instrumentation within the combustor simulator will be used to evaluate the simulator performance and for comparing to model predictions.

Milestones

Milestone	Completion Date	Status
Workplan	03/5/2020	Completed
COE Meeting 1	10/29/2021 - 10/29/2021	Completed
COE Meeting 2	10/26/2022 - 10/28/2022	Completed
COE Meeting 3	10/24/2023	Completed
COE Meeting 4	10/29/2024 - 10/31/2024	Completed
COE Meeting 5	10/14/2025 – 10/16/2025	Completed
Annual Report	12/31/2025	Completed

Major Accomplishments

- Successfully demonstrated improved dirt management for combustor liners through the implementation of a triple-wall cooling design. (Task 2)
- Completed manufacturing of the combustor profile simulator. In addition, more detailed computational predictions of the flowfield to meet the needs of the START facility have been completed including the higher fidelity LES simulations. (Task 3)

Publications

McFerran, K., Thole, K. A., & Lynch, S. P. (2025). Dirt ingestion impacts on cooling within a double-walled combustor liner. *ASME Journal of Turbomachinery, 147*(8), 081019. https://doi.org/10.1115/1.4067464

McFerran, K., Thole, K. A., Lynch, S. P., Boardman, G., Lundgreen, R., Kramer, S., and Joshi, D., (2025), "A Novel Approach to Dirt Mitigation for Combustor Walls," ASME Turbo Expo 2025. https://doi.org/10.1115/GT2025-154071

Schaeffer, C. B., Barringer, M. D., Lynch, S. P., & Thole, K. A. (2025). Influence of dilution and effusion flows in generating variable inlet profiles for a high-pressure turbine. *ASME Journal of Turbomachinery, 147*(3), 031003. https://doi.org/10.1115/1.4066560

Schaeffer, C., Barringer, M., Lynch, S., & Thole, K. (2025, June 15-19). *Comparison of Predicted and Measured Combustor-Relevant Flow Fields* [Poster presentation]. ASME Turbo Expo 2025, Memphis, Tennessee.

Schaeffer, C., Barringer, M., Lynch, S., & Thole, K. (2025, under review) Comparison of Predicted and Measured Combustor-Relevant Flow Fields. *Journal of Turbomachinery*.

Schaeffer, C., Barringer, M., & Thole, K. (2026, June 15-19). *Large Eddy Simulation of a Non-Reacting Profile Simulator for the First-Stage Vane* [Abstract accepted]. ASME Turbo Expo 2026, Milan, Italy.

Outreach Efforts

- Presented periodically to Pratt & Whitney through this joint collaboration.
- Presented the combustor simulator concept to the U.S. Department of Energy, Siemens Energy, Honeywell, and Pratt & Whitney. Industry partners are very supportive of this direction and provide guidance.

Awards

- Dr. Reid Berdanier was elected as an Associate Fellow of the American Institute for Aeronautics and Astronautics (AIAA).
- Dr. Karen Thole was awarded the 2025 Kate Gleason Award from ASME.

Student Involvement

- Chad Schaeffer was a PhD student at Penn State University who led the combustor simulator design effort at Penn State. Chad successfully defended his PhD in August 2025.
- Fabrizzio Vega is a PhD student at the University of Michigan. Fabrizzio completed an internship at NASA Glenn Research Center during Summer 2025, where he performed high-temperature experiments for triple-wall combustor liner samples.
- Dan Strobel (MSME, PSU), Benjamin Bizzak (PhD, PSU) are new graduate students starting Fall 2025 contributing to combustor simulator work at Penn State.
- Peyton Boudinot (U-M) is a new graduate student working on triple-wall combustor liner tests. Peyton was recruited to graduate school following a summer Research Experience for Undergraduates program in the START Lab at Penn State.

Plans for Next Period

- Optimize the multi-wall combustor liner design and evaluate associated heat transfer performance benefits.
- Integrate the profile simulator into the START rig and perform experimental testing.

References

McFerran, K., Thole, K. A., & Lynch, S. P. (2025). Dirt ingestion impacts on cooling within a double-walled combustor liner. *ASME Journal of Turbomachinery, 147*(8), 081019. https://doi.org/10.1115/1.4067464

Schaeffer, C. B., Barringer, M. D., Lynch, S. P., & Thole, K. A. (2025). Influence of dilution and effusion flows in generating variable inlet profiles for a high-pressure turbine. *ASME Journal of Turbomachinery, 147*(3), 031003. https://doi.org/10.1115/1.4066560

Shrager, A. C., Thole, K. A., & Mongillo, D. (2019a). Effects of effusion cooling pattern near the dilution hole for a double-walled combustor liner—Part 1: overall effectiveness measurements. *ASME Journal of Engineering for Gas Turbines and Power, 141*(1), 011022.

Shrager, A. C., Thole, K. A., & Mongillo, D. (2019b). Effects of effusion cooling pattern near the dilution hole for a double-walled combustor liner—Part II: Flowfield measurements. *ASME Journal of Engineering for Gas Turbines and Power, 141*(1), 011023. https://doi.org/10.1115/1.4041153

Disclaimer

This research was funded by the U.S. Federal Aviation Administration Office of Environment and Energy through ASCENT, the FAA Center of Excellence for Alternative Jet Fuels and the Environment, Project 068 through FAA Award Number 13-C-AJFE-PSU-128 under the supervision of Joshua Glottmann. Any opinions, findings, conclusions or recommendations expressed in this material are those of the authors and do not necessarily reflect the views of the FAA.